JOURNAL OF MATERIALS SCIENCE 4 (1969) 450–456

Facetting and Optical Perfection in Czochralski Grown Garnets and Ruby

B. COCKAYNE, M. CHESSWAS, D. B. GASSON
Royal Radar Research Establishment, Malvern, Worcs, UK

Received 13 December 1968

Studies of ruby (Al_2O_3/Cr^{3+}) and rare-earth aluminium garnet single crystals, in particular the mixed garnets formed between $Y_3Al_5O_{12}$ (YAG) and $Dy_3Al_5O_{12}$ (DyAG), have shown that the formation of facets on the solid/liquid interface, which give rise to a strained central core within the crystals, is dependent upon the shape of the solid/liquid interface. Development of the strained and facetted core can be prevented by modifying the growth conditions to produce a flat solid/liquid interface and as a result the optical perfection of the crystals is greatly improved. Certain crystals, e.g. DyAG, grow naturally with a flat interface, and in the present work this has been shown to be due to the optical absorption characteristics of this material. In other materials, e.g. YAG and ruby, the interface shape can be controlled by the rate at which the growing crystal is rotated. The changes in temperature gradient produced in a YAG melt by changes of crystal rotation rate have been measured, and their effect upon crystal perfection is described.

1. Introduction

The rare-earth oxides Y_2O_3, Dy_2O_3, Ho_2O_3, Er_2O_3, Tm_2O_3 and Yb_2O_3 all form congruently melting garnets of the type $R_3Al_5O_{12}$ with Al_2O_3 (R = rare-earth ion). Vertically pulled single crystals of all these garnets except DyAG [1] exhibit a strained central core which is associated with the development of facets, normally of the type {211}, on the growth front of the crystals [2, 3]. This defect is particularly detrimental in laser crystals such as (YAG/Nd^{3+}) as it impairs the optical perfection, and means that laser rods can only be cut from the relatively unstrained outer regions of the crystals. A similar defect occurs in ruby crystals, which develop facets of the type {0001} and {10$\bar{1}$1} [4].

In the present work, the anomalous behaviour of DyAG has been investigated by comparing the strain characteristics, interface shapes and optical absorption spectra of the mixed garnet crystals formed between DyAG and YAG. The information gained from these studies has been used to develop methods by which single crystals of YAG [5] ruby and spinel [6] can be grown without the formation of a strained and facetted core.

2. Experimental Details

The crystals described here were all grown by the vertical pulling (Czochralski) technique using an apparatus already fully described [7]. Melts were prepared from the carefully dried component oxides, and were contained in iridium crucibles heated by an 18 kW radio frequency generator operating at 450 kc/s. The Al_2O_3 was supplied as "Optran" grade material by British Drug Houses Ltd, rare-earth oxides were the highest purity grades available from the American Potash and Chemical Co, and the Cr_2O_3 was Johnson Matthey "Specpure" grade. Crystal growth and rotation rates were in the respective ranges 0.5 to 5 mm/h and 5 to 150 rpm. A gas ambient of argon flowing at 300 cc/min was used for the garnet crystals, but for ruby, 1 vol % of oxygen was added to the growth atmosphere in order to suppress the formation of particles causing optical scattering [7]. In all cases, growth was terminated by quickly raising the crystal clear of the melt, thereby preserving the interfacial growth features.

Crystals for optical studies were cut and polished by standard methods, and the fringe patterns were obtained on a Twyman-Green inter-

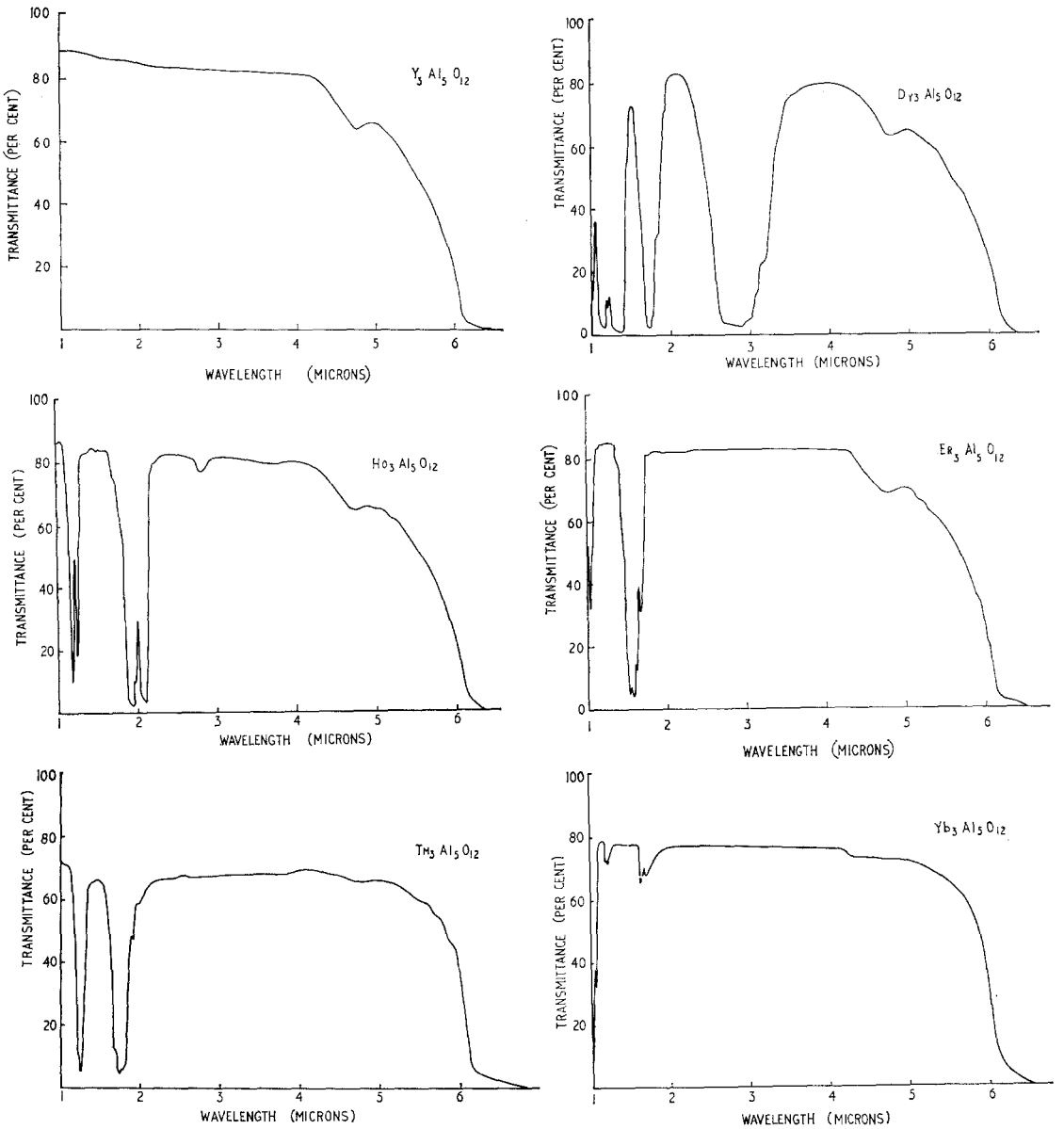

Figure 1 Transmission data for 1 cm thick rare-earth aluminium garnet single crystal sections.

ferometer using a He–Ne gas laser as the light source. Absorption spectra were measured using a spectrophotometric technique.

An Ir–Ir/40% Rh thermocouple was used to measure the melt temperature and this data was recorded on an accurately reverse biased 0 to 1 mV recorder.

3. Results

3.1. The Anomalous Behaviour of DyAG

For the Czochralski growth of single crystal garnet materials, the crystal rotation and growth rates are generally between 5 and 20 rpm and 0.5 and 5 mm/h respectively. It has been confirmed that under these conditions, DyAG is the only rare-earth aluminium garnet which does not exhibit a strained central core. Examination of crystal interfaces shows that DyAG develops a flat solid/liquid interface with respect to the melt, whereas all other garnets form a cone-shaped interface, convex towards the melt, which generally develops facets on areas parallel to

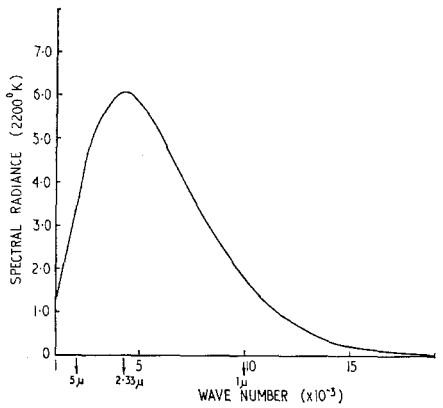

Figure 2 Emission spectrum for a black body radiating at a temperature of 1970° C.

{211} planes. This effect has been verified for DyAG when grown on the orientations {100}, {110} and {111}, and the absence of a strained central core in this material is thus consistent with the inability of {211} facets to form on a flat interface.

Under the standardised growth conditions used here, the factors most likely to affect interface shape are those which alter the heat flow away from the growth front of the crystal. At the melting temperature of the garnets (1970 to 2000° C), heat transfer is almost entirely by radiation, and a crystal growing from its own melt acts as a light pipe through which radiant energy is transmitted from the interface between liquid and solid [8]. Since heat flow from the interface will be restricted by highly absorptive materials, the temperature gradients within the crystal in such a case would be reduced, and the shape of the isotherms modified. The modification would include the freezing isotherm which determines the interface shape, and the absorption characteristics of the crystal should thus influence the shape of its interface during growth. Absorption spectra for the series of rare-earth aluminium garnets studied are shown in fig. 1, and indicate that DyAG is the only member of the series which absorbs radiation extensively in the wavelength range 1 to 6 μm. Comparison with the emission spectrum for a black body radiating at a temperature of 1970° C (fig. 2), corresponding approximately to a garnet melt, shows that a substantial proportion of the radiation emitted by a DyAG melt would be absorbed within the crystal. The main absorption at 2.5 to 3.0 μm corresponds very closely to the peak intensity of the black body emission. This evidence suggests that the absorption characteristics of DyAG account for its anomalous interface shape and freedom from a strained and facetted core. This is further confirmed by the transmission curves, fig. 3, and interface profiles, fig. 4, for a series of DyAG–YAG single crystals grown under identical conditions along {100} axes. The optical absorption due to the Dy^{3+} ion steadily decreases as the molecular proportion of YAG is increased, and the interface shape changes correspondingly from a planar, through a hemispherical to a conical section. In addition, the fraction of radiation absorbed by the mixed garnets in comparison to YAG, $\Delta A/T$ (defined in Appendix 1), varies in a regular manner with both composition (fig. 5) and interface shape (fig. 6). It is also significant that the values of $\Delta A/T$ for HoAG (0.13) and ErAG (0.09) lie within the range where facetted interfaces are formed. These are the only garnets other than DyAG which absorb significantly in the wavelength range 1 to 6 μm.

It must be emphasised that the relationship obtained here between absorption spectra, black body emission from the melt and interface shape is qualitative rather than quantitative, principally because the absorption data were obtained at room temperature. However, absorption should increase with temperature due to line broadening effects produced by increased thermal vibration of the crystal lattice.

3.2. Crystal Rotation Effects

3.2.1. Optical Perfection

A flat solid/liquid interface can be induced artificially on both garnet and ruby crystals growing from their own melts by rotating the crystals at relatively high speeds. The requisite speed is a complex function of crystal and crucible diameter and melt temperature gradient but is generally within the range 100 to 200 rpm for the growth system used here. The flat interface inhibits facet formation and allows the growth of relatively strain-free crystals with a high degree of optical perfection. This effect is demonstrated in fig. 7 which compares the Twyman Green interference patterns for two *a*-axis ruby crystals both containing 0.05 at. % Cr, but grown at different rates of rotation. Fig. 7a is the pattern for a crystal with a cone-shaped interface which developed a $\{10\bar{1}1\}$ type facet,

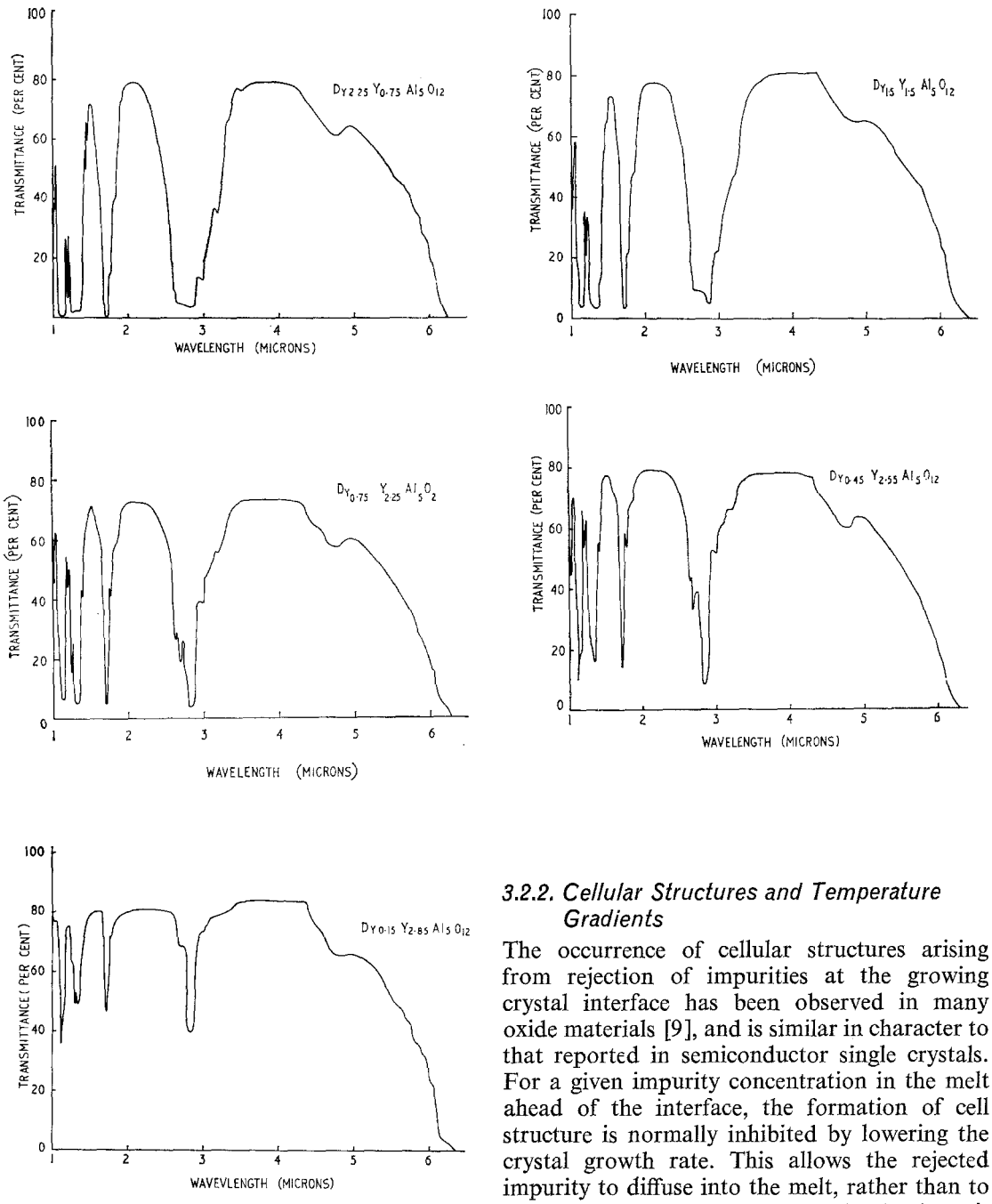

Figure 3 Transmission data for 1 cm thick DyAG–YAG single crystal sections.

whilst fig. 7b shows the improved perfection in a facet free crystal grown with a planar interface at a rotation speed of 150 rpm. These results are thus consistent with data on YAG single crystals published elsewhere by the present authors [5].

3.2.2. *Cellular Structures and Temperature Gradients*

The occurrence of cellular structures arising from rejection of impurities at the growing crystal interface has been observed in many oxide materials [9], and is similar in character to that reported in semiconductor single crystals. For a given impurity concentration in the melt ahead of the interface, the formation of cell structure is normally inhibited by lowering the crystal growth rate. This allows the rejected impurity to diffuse into the melt, rather than to increase in concentration to a level where it causes sufficient supercooling for the interface to change from a planar to a cellular morphology. Alternatively, the temperature gradient in the melt can be increased to reduce the effective supercooling [10]. One consequence of the high rotation speeds used in the present work is that the temperature gredients in the melt are in fact lowered (table I), thereby enhancing the forma-

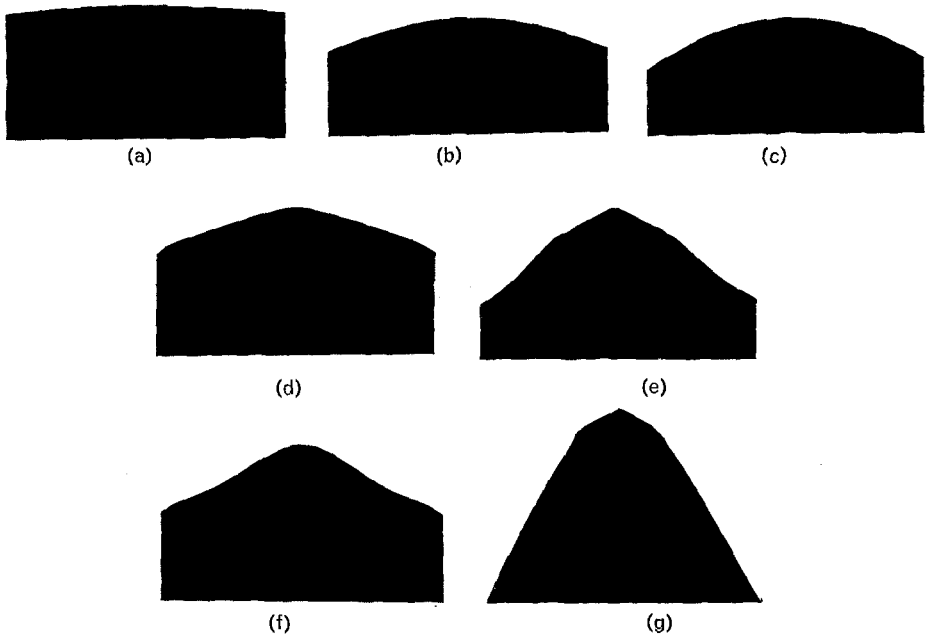

Figure 4 Interface profiles for DyAG–YAG single crystals grown under identical conditions (× 5). (a) $Dy_3Al_5O_{12}$, (b) $Dy_{2\cdot25}Y_{0\cdot75}Al_5O_{12}$, (c) $Dy_{1\cdot5}Y_{1\cdot5}Al_5O_{12}$, (d) $Dy_{1\cdot75}Y_{2\cdot25}Al_5O_{12}$, (e) $Dy_{0\cdot45}Y_{2\cdot55}Al_5O_{12}$, (f) $Dy_{0\cdot15}Y_{2\cdot85}Al_5O_{12}$, (g) $Y_3Al_5O_{12}$.

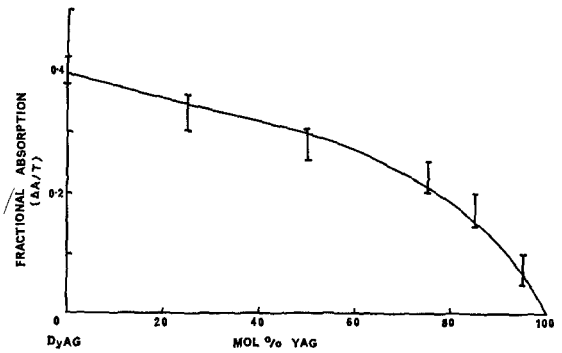

Figure 5 The variation of $\Delta A/T$ with composition in the DyAG–YAG system.

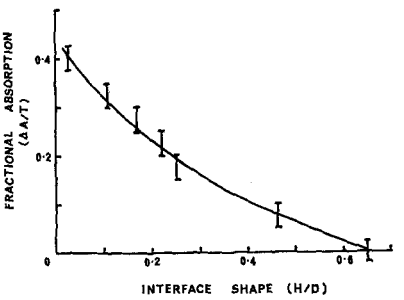

Figure 6 The variation of $\Delta A/T$ with interface shape in the DyAG–YAG system (see Appendix 2).

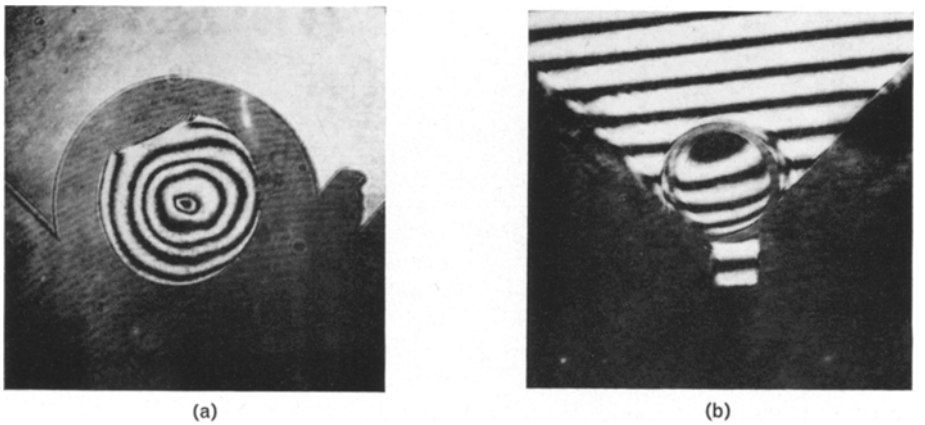

Figure 7 Twyman-Green interference fringes observed through 5 cm long ruby single crystals containing 0.05 at.% Cr. (a) grown at 50 rpm (× 2), (b) grown at 150 rpm (× 1.5).

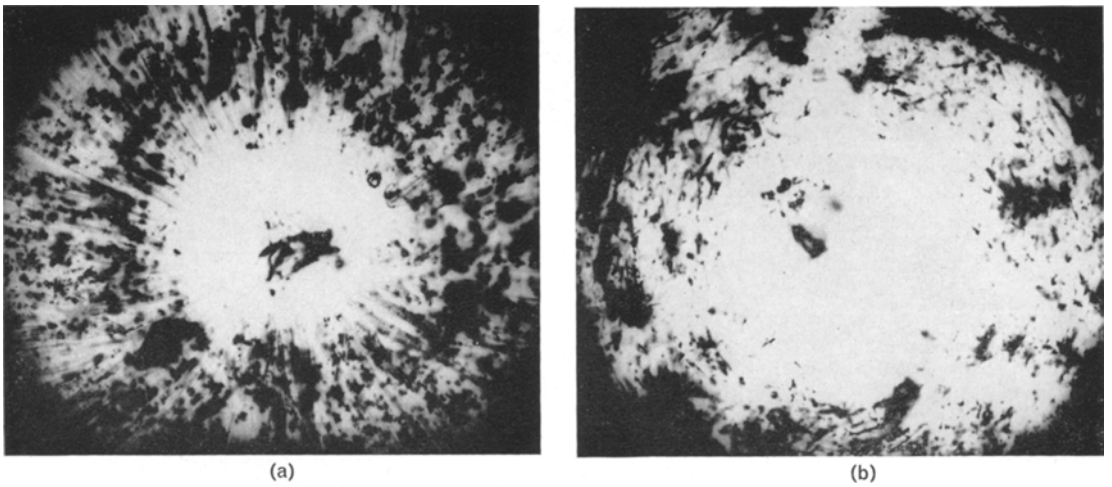

(a) (b)

(c)

Figure 8 Cellular structure observed in YAG single crystals containing Nd and grown at (a) 10 rpm, (b) 60 rpm, (c) 120 rpm (× 11).

tion of cellular structures. In order to avoid these structures, the growth rate has to be correspondingly decreased, and for YAG containing 1 at. % Nd, the rate of growth must be less than 0.2 mm/h at a rotation speed of 150 rpm. The values quoted in table I are the range of gradients detected in five independent measurements at each rotation speed. They represent a general trend rather than precise data, as quite wide variations were observed in measurements made under apparently identical conditions.

The morphology of the cellular structure is markedly dependent upon the rate of rotation during growth, as demonstrated in YAG by fig. 8. At low rotation rates, a radial spoke-like

TABLE I

Crystal rotation speed (rpm)	Temp. grad. in YAG melt in the region 0 to 6 mm below the interface of a growing crystal (° C/cm)
50	91 ± 10
100	57 ± 15
150	30 ± 15

structure is adopted, which changes first to a circumferential pattern and subsequently to a vortex-like structure as the rate of rotation is progressively increased. This suggests that the morphology of the cellular structure is related to the fluid flow within the melt, which is predominantly a convective flow, directed radially towards the crucible centre when the crystal is either stationary or rotating slowly. When the crystal rotation is increased, the flow pattern first becomes diffuse in the volume of melt adjacent to the crystal. As the rate of rotation is increased further, the flow assumes a spiral or vortex-like pattern as the hydrodynamic flow induced by the crystal becomes predominant over the opposing convective flow [11].

The effects described and shown in fig. 8 are slightly masked by the presence of facets. The absence of marked cell structure on the facetted regions is nevertheless consistent with the generally acknowledged difficulty of initiating new growth on facets [12]. Fig. 8c shows that regions of the interface which are parallel to the facetting {211} planes move away from the

crystal centre as the interface becomes less convex towards the melt.

Crystals containing cellular structure to the extent shown in fig. 8 generally have a less conical interface than crystals entirely free from this defect. It appears possible therefore for cellular structures to contribute to the total amount of radiation absorbed within a growing crystal.

4. Conclusions

The studies described here show that the rate at which a crystal rotates during the Czochralski growth of oxides has a marked influence upon crystal quality and that crystal rotation rate cannot be regarded as an arbitrary parameter. Crystals with a high degree of perfection can only be prepared if the rotation rate is optimised in conjunction with the other principal control parameters, namely growth rate and temperature gradient.

Acknowledgement

The authors wish to acknowledge Mr M. Bishop-Bailey for his assistance with some of the crystal growth.

This paper is published by permission of The Controller, HMSO.

Appendix 1

The fraction of radiation absorbed in DyAG–YAG crystal sections (ΔA) compared with the total transmitted by YAG (T) at wavelength λ is equal to $(I_{YAG} - I_{DyAG})/I_{YAG}$ where I is the transmitted intensity. As the incident intensity varies with wavelength, I varies in a corresponding manner and the total intensity transmitted between wavelengths λ_1 and λ_2 is given by

$$\Sigma I = \int_{\lambda}^{\lambda} I_\gamma \, e^{-\alpha_\lambda x} \cdot (1 - R)^2 \, d\lambda$$

where x is the specimen thickness, α_λ is the absorption coefficient at wavelength λ, R is the reflection coefficient and I_λ is the spectral radiance emitted by a black body at a temperature of 1970°C.

Hence $\Delta A/T$ becomes equal to $(\Sigma I_{(YAG)} - \Sigma I_{(DyAG)})/\Sigma I_{(YAG)}$.

However, $x = 1$, $R_{YAG} \simeq R_{DyAG}$, and as $\alpha_{\lambda(DyAG)}$ is determined with respect to YAG, $\alpha_{\lambda(YAG)}$ automatically becomes zero. $\Delta A/T$ therefore becomes equal to

$$\frac{\int_{\lambda_1}^{\lambda_2} I_\lambda \cdot d_\lambda - \int_{\lambda_1}^{\lambda_2} I_\lambda \cdot e^{-\alpha_\lambda (DyAG)} \, d\lambda}{\int_{\lambda_1}^{\lambda_2} I_\lambda \cdot d\lambda}$$

which is the factor plotted in figs. 5 and 6.

Appendix 2

For the purposes of the present work, the interface shape is defined as the aspect ratio (height, H/crystal diameter, D) of the partial spherical or cone-shaped section through the centre of the decanted crystal interface. Efforts were made to grow all crystals with $D = 1$ cm; the tolerance achieved was $\pm$ 0.2 cm.

References

1. F. R. CHARVAT and R. M. YOUMANS, *Bull. Amer. Ceram. Soc.* **44** (1965) 409.
2. W. BARDSLEY and B. COCKAYNE, Crystal Growth (Suppl. to *J. Phys. Chem. Sol.*) (1967) 109.
3. J. BASTERFIELD, M. J. PRESCOTT, and B. COCKAYNE, *J. Materials Sci.* **3** (1968) 33.
4. F. R. CHARVAT, J. C. SMITH, and O. H. NESTOR, Crystal Growth (Suppl. to *J. Phys. Chem. Sol.*) (1967) 45.
5. B. COCKAYNE, M. CHESSWAS, and D. B. GASSON, *J. Materials Sci.* **3** (1968) 224.
6. B. COCKAYNE, M. CHESSWAS, P. J. BORN, and J. D. FILBY, *ibid* **4** (1969) 236.
7. B. COCKAYNE, M. CHESSWAS, and D. B. GASSON, *ibid* **2** (1967) 7.
8. K. NASSAU and A. M. BROYER, *J. Amer. Ceram. Soc.* **45** (1962) 1.
9. B. COCKAYNE, *J. Crystal Growth* **3** (1968) 60.
10. D. T. J. HURLE, *Sol. State Electron* **3** (1961) 37.
11. D. S. ROBERTSON, *Brit. J. Appl. Phys.* **17** (1966) 1047.
12. J. B. MULLIN and K. F. HULME, *J. Phys. Chem. Solids* **17** (1960) 1.